Supporting Information

Toh et al. 10.1073/pnas.0911535107

SI Text

SI Materials and Methods. ***Sample preparation.*** The detailed preparation of RpBphP2 and RpBphP3 bacteriophytochrome proteins and their mutants were described previously (1). For H/D exchange experiments, the proteins were dissolved in D_2O buffer (20 mM Tris · HCl, pD 8 at room temperature). H/D exchange was carried out by removing the H_2O buffer by using an ultracentrifuge and then adding the D_2O buffer to dilute the protein concentration. These procedures were repeated for at least 6 times to minimize the content of the H_2O buffer. The deuterated proteins were prepared at least 24 hours prior to the experiments. On the day of the experiments, the samples (in D_2O buffer) were further diluted by adding the D_2O buffer.

Femtosecond transient absorption spectroscopy. Femtosecond transient absorption experiments were performed by using an amplified Ti:sapphire-based laser setup. A seed pulse from a diode-pumped oscillator (Coherent Vitesse, 800 nm, 80 MHz, 100 fs) is amplified to 2.5 W by using a Nd:YLF high-power pump laser (Coherent Evolution-20, 527 nm, 1 kHz). The Ti:sapphire-based amplifier (Coherent Legend-USP) incorporates chirped pulse amplification and a stretcher/compressor combination to deliver sub-50-fs pulses, with a center wavelength at 800 nm and a bandwidth of 30 nm (FWHM) at a repetition rate of 1 kHz. The beam is guided into an optical parametric amplification setup (Coherent OpeRA), which converts the pump-laser output to a tunable pair of outputs: the signal (1,150–1,600 nm) and the idler (1,600–2,630 nm). To generate a 680-nm pump beam, the signal at 1,360 nm was frequency-doubled in a nonlinear crystal. A small fraction of the initial 800-nm beam was used to generate the white-light probe light by using a sapphire crystal. The protein solution sample was contained in a quartz flow cuvette with a 2-mm path length. A diaphragm metering pump model STEPDOS 03S from KNF Neuberger, Inc. is used to flow the fresh sample in the cuvette from an external cuvette with an ~3–4 mL sample. The external cuvette is constantly under illumination by a 750- (P2) or 650-nm LED light (P3) so that the light-activated sample is brought to the ground state before feeding into the flow cuvette. Alternatively, a 2-mm quartz cuvette is used without flowing but attached to a high frequency shaker, and with direct illumination of a 750- or 650-nm LED. The flow and shaking cuvette methods gave identical results. The sample used has an OD of about 0.2–0.4/(2 mm) at the excitation wavelength. Both the pump light of 680 nm with energy of 200–400 nJ (generated from the optical parametric amplifier, second harmonic generation) and the probe light are focused and overlapped at the sample in the cuvette. The probe light was focused on the entrance slit of a spectrograph, spectrally dispersed, and projected on a 256 diode-array detector. The spectral resolution was 1.2 nm. A reference data using water is collected by using the same experimental conditions. This reference data is used to correct artifacts caused by cross-phase modulation near time zero because of pulse interaction between the probe and the pump in the solvent and cuvette windows.

Time-resolved fluorescence spectroscopy. Time-resolved fluorescence measurements were carried out by using a streak camera setup described earlier (2). An integrated Ti-sapphire oscillator (Coherent Vitesse) produced pulses of 800 nm with 100 fs duration at 80 MHz repetition rate. This beam is directed into a regenerative amplifier (Coherent RegA) operating rate between 48 and 128 kHz and then fed into an optical parametric amplifier (CoherentOPA). The OPA is able to generate excitation (pump) pulses from 470 to 720 nm. The synchronization of the camera with the frequency of the pulses is achieved through monitoring of a split of the initial 800-nm beam by using a PIN diode. The pump light is focused on a 1-cm path-length quartz cuvette that is placed on top of a magnetic stirrer. The sample with about 0.1 OD/cm is pumped by the 681-nm laser beam, with background illumination using a 750- or 645-nm LED in order to bring the light-activated sample to the ground state. The emission from the sample is collected at a right angle with respect to the pump beam and focused into the slit and grating by using an achromatic lens. A sheet polarizer is used to adjust the magic angle (54.7°, with respect to the polarization angle of the pump beam) of the collected emission. The dispersed light is converted to electrons at the photocathode and time-resolved by using a sweep circuit that varies the voltage applied to sweep electrodes. A microchannel plate is used to amplify the electron signal, and this signal is projected to a phosphor screen and then is detected by the camera. Two sets of data for one sample are collected, with a time range up to 200 ps (time range 1) and 2 ns (time range 4), at time resolutions of 5 and 21 ps, respectively.

Data analysis. Femtosecond transient absorption data were globally analyzed through the spectra range in the data. The global analysis gives an idea of the number of possible intermediate states that is evolving in time, in a sequential manner. This sequential model assumes increasing lifetimes in the subsequent intermediate states. The spectra estimated by the analysis are termed as evolution-associated difference spectra (EADS). EADS does not necessary represent the right kinetic model for the system because a number of energy and charge transfer processes might be happening in parallel. Therefore, a kinetic model that includes processes happening in series and in parallel must be employed. This analysis is termed as a target analysis and is used in addition to the global analysis. The spectra produced by target analysis are termed species-associated difference spectra (SADS). In this study, we analyzed sample data in H_2O and D_2O simultaneously and routinely found a higher yield of the Lumi-R primary product state in D_2O. To correlate the decay rate constant with the lifetime, we can utilize the formula below:

$$I(t) = I_0 e^{-t/\tau},$$

where

$$\frac{1}{\tau} = \sum_i \theta_i$$

and t is time, τ is the lifetime of the state, I_0 is the initial population of the state at $t = 0$, and θ_i are the rates for each decay pathway. Details of this method and analysis can be found elsewhere (3).

In time-resolved fluorescence measurements, an independent exponential decay scheme is assumed that produces the decay-associated spectra (DAS). The DAS in time-resolved data is generally used to show the multiexponential decay of the excited states.

Fluorescence quantum yield experiments. Fluorescence quantum yield measurements were performed by using a commercial fluorometer with right-angle detection geometry (Jobin-Yvon). Cy5 was used as a fluorescence quantum yield standard

($F_F = 0.27$). The samples were contained in a cuvette with 1-cm path length in the excitation direction and 0.4-cm path length in the detection direction. The absorbance of Bph and reference samples was adjusted to similar values of less than 0.03 per cm; fluorescence intensities were corrected for the number of absorbed photons. The excitation density was kept low to avoid photoconversion of the Bph samples. The fluorescence spectra were corrected for the wavelength sensitivity of the detection system and converted to an energy scale, thereby correcting the change in bandpass through the relation $I(n) = l^2 I(l)$ (4). The fluorescence spectra were recorded and integrated up to 850 nm.

1. Yang X, Stojkovic EA, Kuk J, Moffat K (2007) Crystal structure of the chromophore binding domain of an unusual bacteriophytochrome, RpBphP3, reveals residues that modulate photoconversion. *Proc Natl Acad Sci USA* 104:12571–12576.
2. Gobets B, et al. (2001) Time-resolved fluorescence emission measurements of photosystem I particles of various cyanobacteria: A unified compartmental model. *Biophys J* 81:407–424.
3. van Stokkum IHM, Larsen DS, van Grondelle R (2004) Global and target analysis of time-resolved spectra. *Biochim Biophys Acta (Bioenerg)* 1657:82–104.
4. Lackowicz JR (2006) *The Principles of Fluorescence Spectroscopy* (Plenum Press, New York).

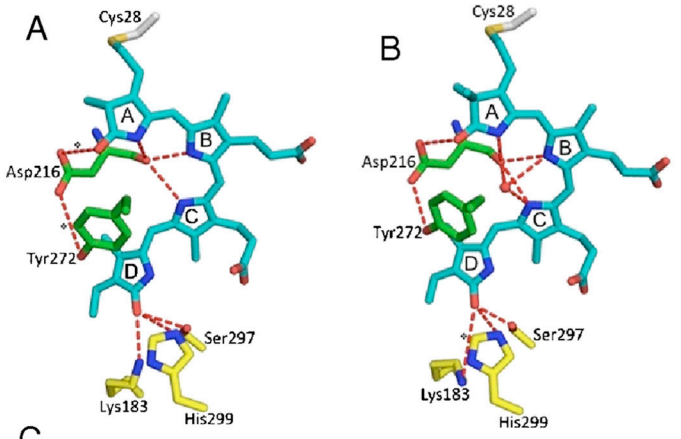

C

```
          183          216   272                        297
RpBphP3   -KVYQFA-HFPSSDIPAQ-YMVNMGMHAAMSISIVRDNRLWGMISCHNL-
RpBphP2   -MIYRFA-HFPASDIPAQ-YMRNIGMHGTMSISILRGERLWGLIACHHR-
DrBphP    -MAYRFR-RFPASDIPAQ-YLRNMGVGSSLSVSVVVGGQLWGLIACHHQ-
AtBphP1   -LIYDFG-RFPAGDIPPQ-YMRNMGTAASMSVSIVVNGALWGLIACHHA-
PaBphP    -MLYKFA-RYPASDIPAQ-YLTNMGVRASMSISIVVGGKLWGLFSCHHM-
Cph1      -MLYRFD-HYPESDIPQP-YLKNMGVGASLTISLIKDGHLWGLIACHHQ-
```

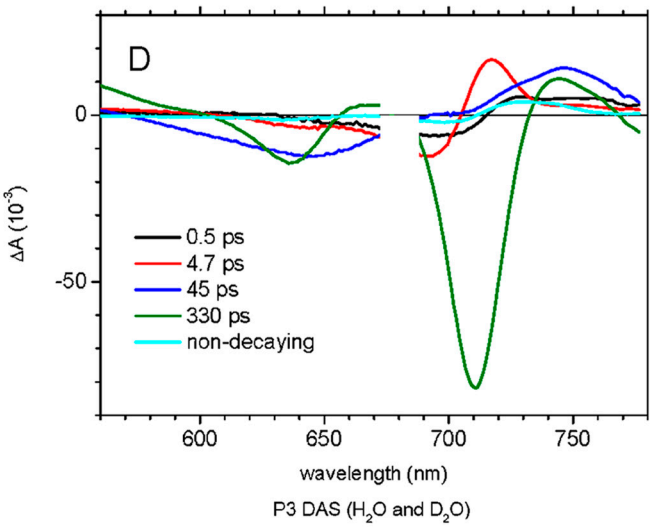

P3 DAS (H_2O and D_2O)

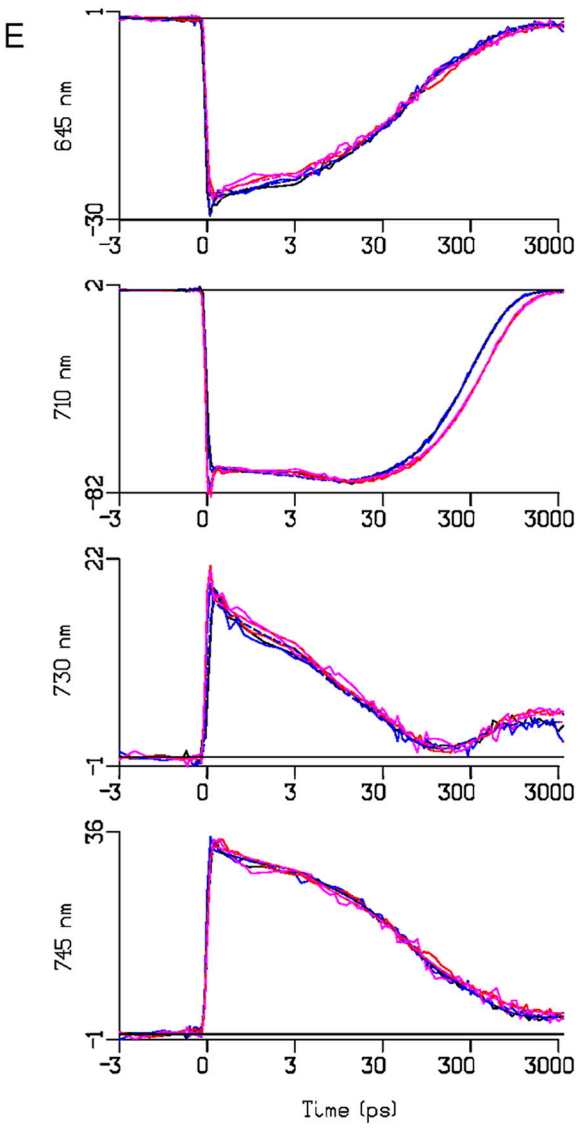

P3 fluorescence lifetime traces at 717 nm

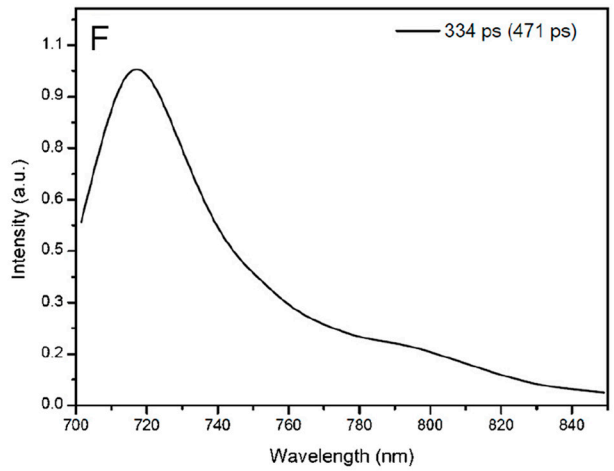

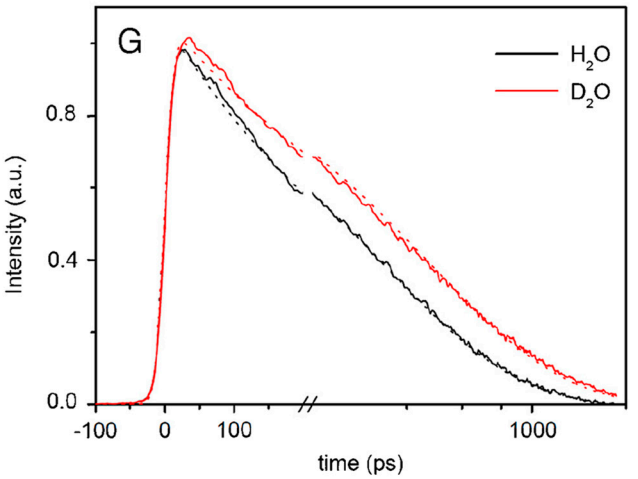

Fig. S1. Three-dimensional structure and results of ultrafast transient absorption and time-resolved fluorescence spectroscopy on *Rhodopseudomonas palustris* P3. (*A*) The biliverdin (BV) binding site in the x-ray structure of *R. palustris* P3 (monomer II). (*B*) The same as *A* for P3 monomer I—weak interactions that fall out of range for H-bond distances between two monomers are indicated with small crosses. (*C*) Partial protein sequence alignment of P3 and P2, *Deinococcus* DrBph, *Agrobacterium* AtBphP1, *Pseudomonas* PaBphP, and *Synechocystis* Cph1. (*D*) Decay-associated difference spectra (DADS) that follow from a global analysis of ultrafast transient absorption data of P3 in H_2O. The 0.5 ps DADS (*Black Line*) represents an overall redshift of the bleach/stimulated emission band. It has an overall low amplitude and will not be discussed further here. The 4.7 DADS (*Red Line*) is overall conservative and shows a negative band at around 690 and a positive band at 719 nm. The positive lobe can be regarded as a decay of absorption or a rise of stimulated emission. The negative lobe can be regarded as a rise of absorption or a decay of stimulated emission. Given that the positive lobe in the 4.7-ps component corresponds to the fluorescence emission maximum, the 4.7-ps process can either be interpreted as a redshift of stimulated emission, as a blueshift of excited-state absorption, or as a combination of both. The 45-ps DADS (*Blue Line*) is conservative with almost equal intensity in its positive (740 nm) and negative (640 nm) lobes: The 45-ps decay of absorption at 740 nm is accompanied with a diminishing of the apparent bleach near 640 nm, which is consistent with a rise of excited-state absorption at the latter wavelength. Thus, the 45-ps component represents a blueshift of excited-state absorption. There is no evidence that the 4- or 45-ps components represent excited-state decay, and we conclude that on the 4.7- and 45-ps time scales, excited BV evolves on the excited-state potential energy surface changing its Franck–Condon overlap with higher-lying excited states or with the ground state, likely related to structural evolution of BV (compare, e.g., with isomerization reactions in small organic molecules and bacteriorhodopsin in refs. 1–3). Given the (presumably) modest Huang–Rhys factor for vibronic coupling of BV and our excitation conditions in the main Q band of BV, vibrational cooling is unlikely to contribute to these processes (4). Importantly, the 4.7- and 45-ps DADS do not show any loss of ground-state bleach or stimulated emission features and consequently do not involve loss of excited-state population. (*E*) Kinetic traces at selected wavelengths of P3 in H_2O (*Blue and Black Lines*) and D_2O (*Red and Magenta Lines*). The blue and black lines denote two datasets in H_2O, whereas the red and magenta lines denote two datasets in D_2O. The dashed lines denote the result from the target analysis procedure. The time axis is linear up to 3 ps and logarithmic thereafter. (*F*) Time-resolved fluorescence of P3 in H_2O and D_2O. Decay-associated spectrum that results from a simultaneous global analysis of the time-resolved data in H_2O and D_2O. One decay component with an emission peak at 717 nm and with a lifetime of 334 ps in H_2O and 471 ps in D_2O is sufficient for an adequate fit; (*G*) fluorescence kinetic traces at 717 nm in H_2O (*Solid Black*) and D_2O (*Solid Red*), along with the result of the fit (*Dashed Lines*). Note that the time axis is linear up to 200 ps and logarithmic thereafter.

1 Lednev IK, et al. (1998) Femtosecond time-resolved UV-visible absorption spectroscopy of transazobenzene: Dependence on excitation wavelength. *Chem Phys Lett* 290:68–74.
2 Mathies RA, Lin SW, Ames JB, Pollard WT (1991) From femtoseconds to biology—Mechanism of bacteriorhodopsins light-driven proton pump. *Annu Rev Biophys Biophys Chem* 20:491–518.
3 Aberg U, et al. (1994) Femtosecond spectral evolution monitoring the bond-twisting event in barrierless isomerization in solution. *Chem Phys* 183:269–288.
4 Struve WS (1995) Vibrational equilibration in absorption difference spectra of chlorophyll. *Biophys J* 69:2739–2744.

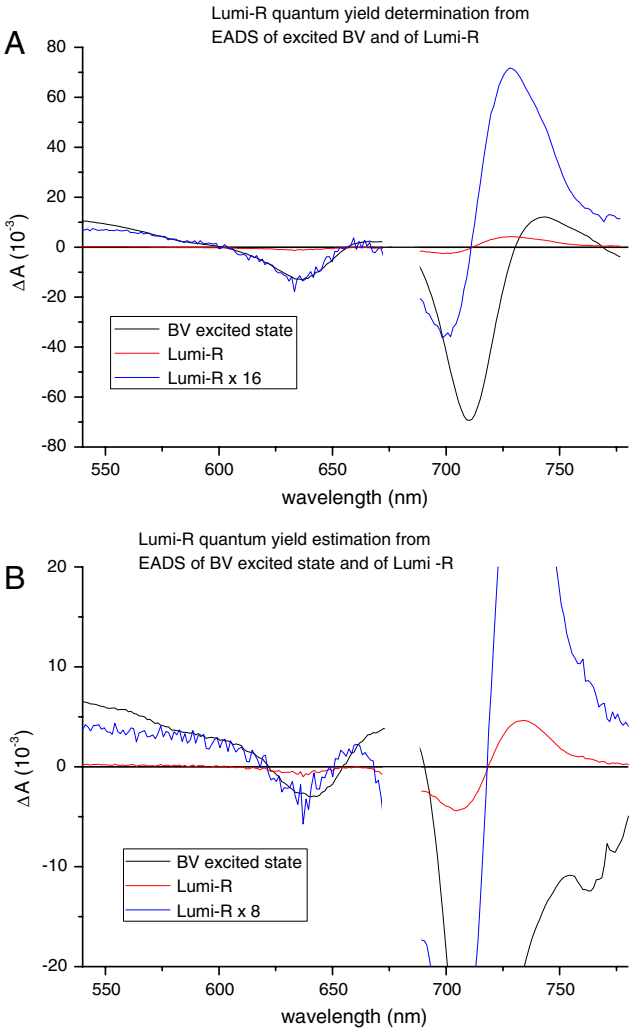

Fig. S2. Estimation of the Lumi-R quantum yield in *R. palustris* P3 and P2. (*A*) Lumi-R quantum yield estimation for *R. palustris* P3 through the bleach amplitude of the Pr vibronic band at 635 nm. The EADS are reproduced from Fig. 2*A* in the main text: 330 ps EADS (black), Lumi-R EADS (red). The blue line denotes the Lumi-R EADS scaled 16 times plus addition of a small baseline to overlay it with the BV excited-state EADS. (*B*) Lumi-R quantum yield estimation for *R. palustris* P2 through the bleach amplitude of the Pr vibronic band at 635 nm. The EADS are reproduced from Fig. 3*B* in the main text: 43 ps EADS (black), Lumi-R EADS (red). The blue line denotes the Lumi-R EADS scaled 8 times plus addition of a small baseline to overlay it with the BV excited-state EADS.

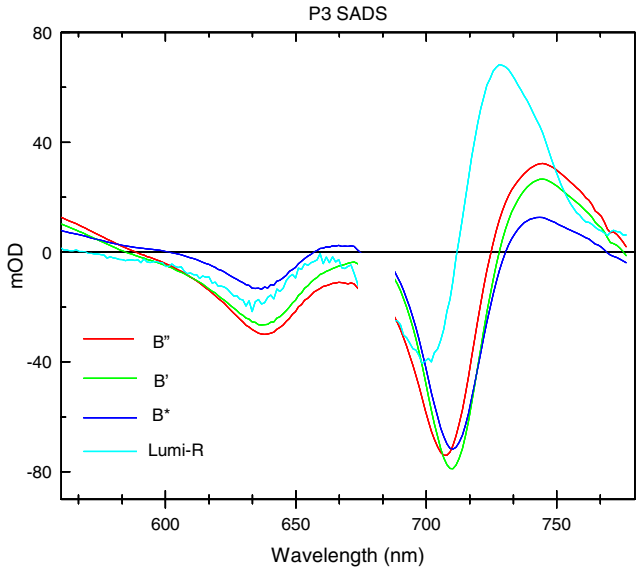

Fig. S3. Target analysis of *R. palustris* P3. SADS that result from the target analysis by simultaneously analyzing the P3 data dissolved in H_2O and D_2O.

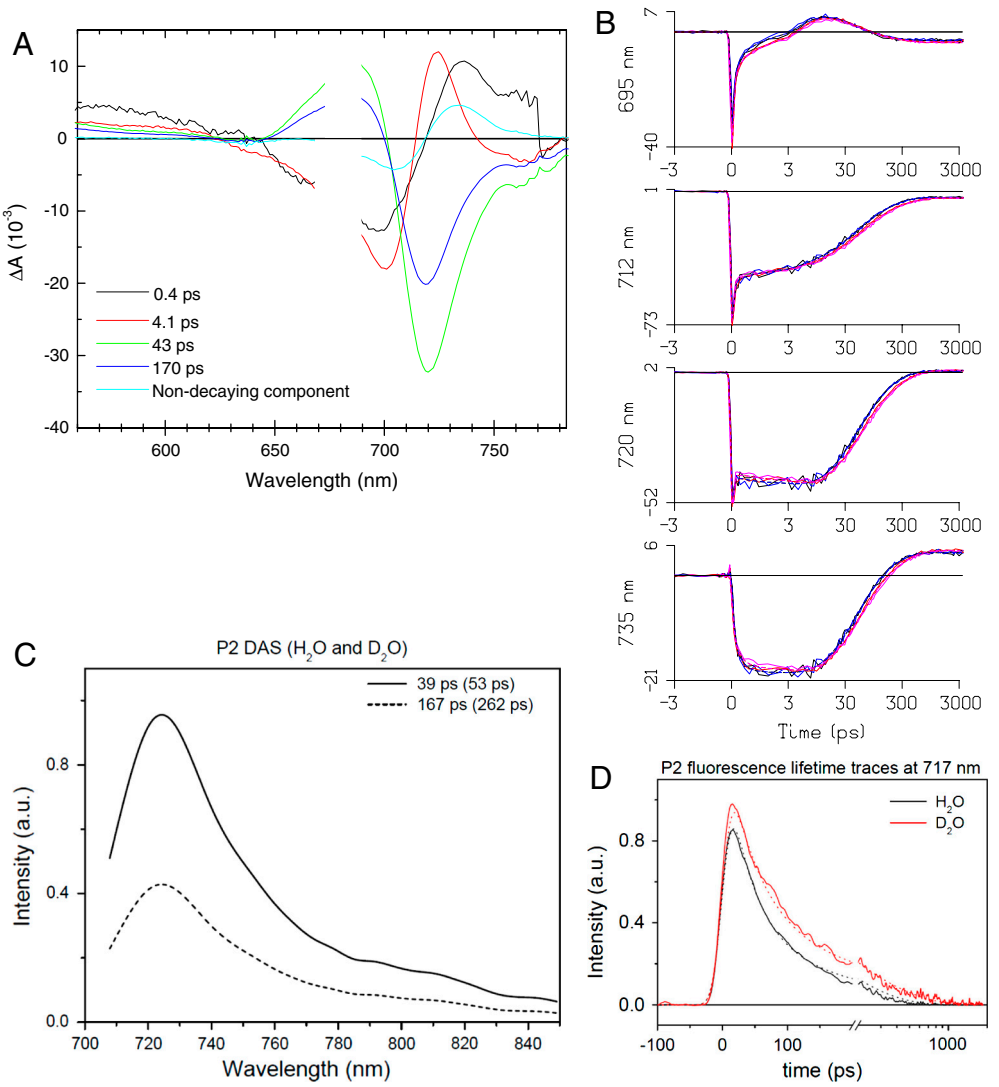

Fig. S4. Ultrafast transient absorption and time-resolved fluorescence spectroscopy on *R. palustris* P2. (*A*) DADS that result from a simultaneous global analysis of the transient absorption data in H_2O and D_2O. The 0.4-ps DADS (*Black Line*) is overall more or less conservative and shows a negative band at around 695 and a positive band at 735 nm. The 4.1-ps DADS (*Red Line*) has a negative band at 695 nm, a positive band at 725 nm, and a small negative band at 750 nm. It represents an overall redshift of the difference spectrum, with the negative band at 750 denoting either a small rise of absorption or a small loss of stimulated emission. There is no loss of ground-state bleach in the 0.4- and 4.1-ps components, which indicates that no excited-state decay takes place. Most likely, the 0.4- and 4.1-ps components represent evolution of excited BV on the excited-state potential energy surface changing its Franck–Condon overlap with higher-lying excited states or with the ground state. Note that the shapes of the 43- (*Green Line*) and 170-ps (*Blue Line*) DADS are similar. Both correspond to excited-state decay and Lumi-R production. (*B*) Kinetic traces at selected wavelengths of P2 in H_2O (*Blue and Black Lines*) and D_2O (*Red and Magenta Lines*). The blue and black lines denote two datasets in H_2O, whereas the red and magenta lines denote two datasets in D_2O. The dashed lines denote the result from the target analysis procedure. The time axis is linear up to 3 ps and logarithmic thereafter. (*C*) Decay-associated spectra that follow from global analysis of time-resolved fluorescence of P2 in H_2O and D_2O; (*D*) fluorescence kinetic traces at 717 nm in H_2O (*Solid Black*) and D_2O (*Solid Red*), along with the result of the fit (*Dashed Lines*). Note that the time axis is linear up to 200 ps and logarithmic thereafter.

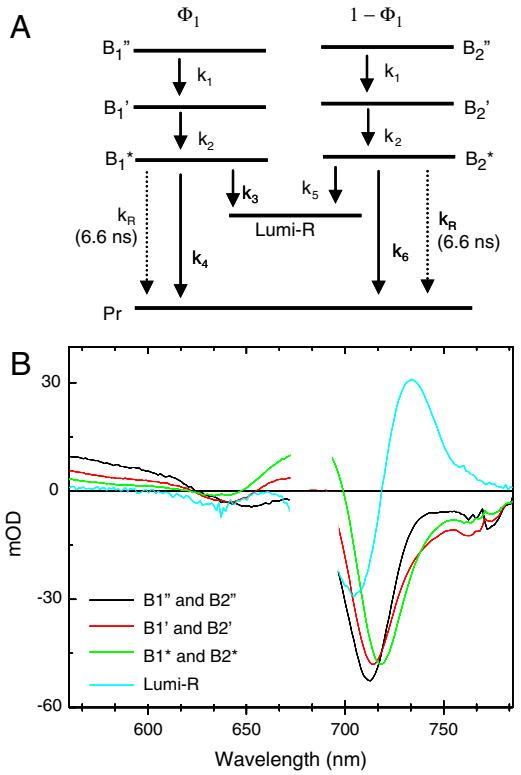

Fig. S5. Target analysis of *R. palustris* P2. (*A*) Kinetic scheme used for target analysis of P2. To take ground-state heterogeneity into account, two excited-state relaxation branches were introduced into the kinetic model: $B_1'' \rightarrow B_1' \rightarrow B_1^*$ and $B_2'' \rightarrow B_2' \rightarrow B_2^*$, populated with fraction Φ_1 and 1-Φ_1, respectively. The initially prepared excited states $B_{1,2}''$ evolve to $B_{1,2}'$ with rate constant k_1. $B_{1,2}'$ evolve to $B_{1,2}^*$ with rate constant k_2. k_1 and k_2 correspond to the ~0.3- and ~4-ps processes, respectively. B_1^* represents the fast excited-state decay channel (~43 ps), whereas B_2^* corresponds to the slow decay channel (~170 ps). B_1^* forms Lumi-R by rate constant k_3 and deactivates to the ground state with k_4. For B_2^* these rate constants are k_5 and k_6, respectively. As for P3, a radiative decay constant $k_R = (6.6\ \text{ns})^{-1}$ is added. In the simultaneous analysis, the SADS of the datasets in H_2O and D_2O are required to remain identical. In addition, the SADS of B_1'' and B_2'', of B_1' and B_2', and of B_1^* and B_2^* are set equal. The rate constants k_{1-6} are allowed to vary freely except k_4, which is fixed to arrive at the correct Lumi-R quantum yield of 0.13 (see Fig. S3 and the discussion in the main text for P3). Also, k_5 was required to be identical in H_2O and D_2O, which was necessary to restrain the parameter space. (*B*) SADS that result from the target analysis by simultaneously analyzing the P2 data dissolved in H_2O and D_2O.

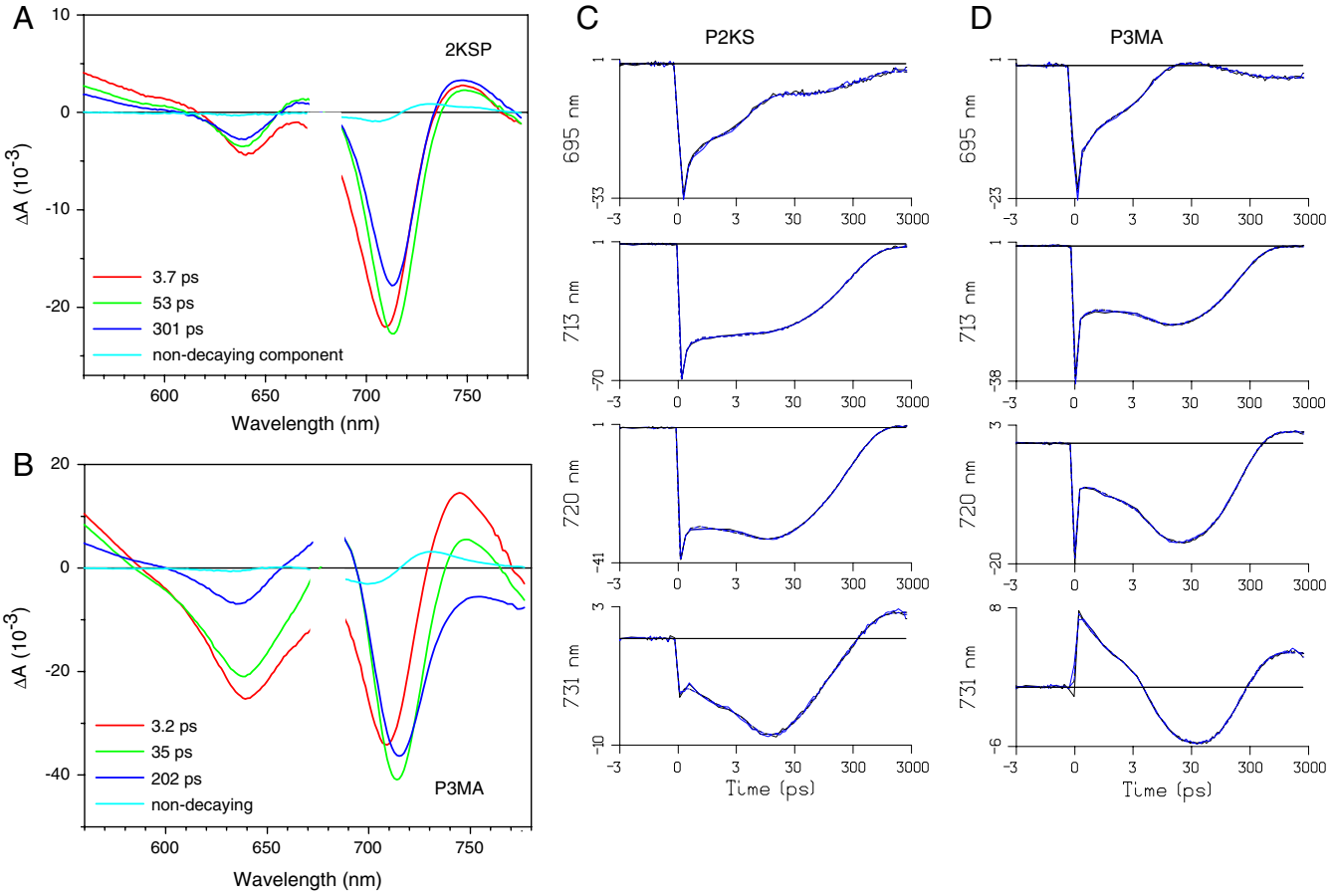

Fig. S6. Transient absorption spectroscopy of the P2KS and P2MA mutants. (*A*) EADS that follow from a global analysis of transient absorption experiments on the P2KS mutant. The excitation wavelength was 680 nm. The quantum yield of Lumi-R formation in P2KS is estimated through comparison of the bleach at 635 nm of the relaxed BV singlet excited state (301-ps component, *Blue Line*) and that of Lumi-R (*Cyan Line*). The Lumi-R quantum yield is estimated at ~0.07. (*B*) EADS for the P3MA mutant. The Lumi-R quantum yield of the P3MA mutant cannot be estimated from its 635-nm band because the BV excited-state spectra look unusual in this wavelength region. However, given that from ~680 to 760 nm the spectra of P3MA (202-ps EADS) and wild-type P2 (43-ps EADS, Fig. 3*D* in the main text) have similar shapes, the relative yields may be estimated by determining the ratio of ground-state bleach at 707 nm in the BV excited state and the Lumi-R absorption at 727 nm. These ratios are in fact similar: In wild-type P2, this ratio is 1:10.3, whereas in the P3MA mutant it is 1:11.5. This observation implies that the Lumi-R quantum yield in P3MA amounts to ~12%, essentially the same as in P2 wild type and significantly higher than in P3 wild type. (*C*) Kinetic traces of the P2KS mutant at selected wavelengths (*Blue Lines*), along with the result of the global analysis procedure (*Black Lines*); (*D*) kinetic traces of the P3MA mutant at selected wavelengths (*Blue Lines*), along with the result of the global analysis procedure (*Black Lines*)

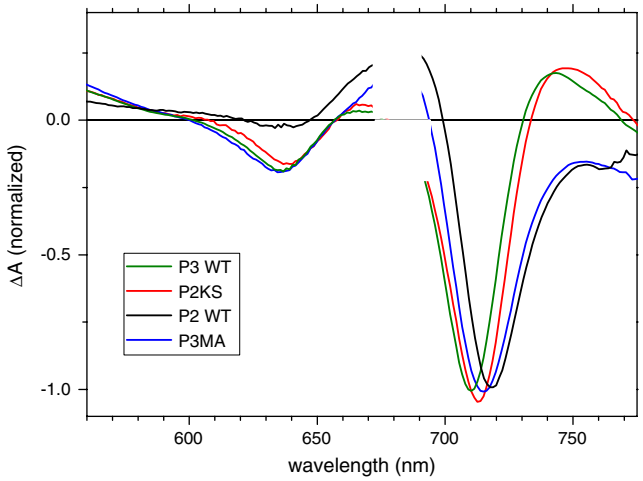

Fig. S7. Difference spectra of the relaxed BV excited state in P3 wild type (*Green Line*), the P2KS mutant (*Red Line*), P2 wild type (*Black Line*), and the P3MA mutant (*Blue Line*). The spectra were reproduced from the EADS of Fig. 2*A* (P3 wild type, 330-ps EADS), Fig. 2*D* (P2 wild type, 43-ps EADS), Fig. S6*A* (P2KS, 301-ps EADS), and Fig. S6*B* (P3MA, 202 ps EADS). In P3 and the P2KS mutant, ESA is observed at the red side of the ground-state bleach at 745 nm. This is different in P2 and the P3MA mutant, where ESA is seen at 680 nm and stimulated emission near 745 nm. The spectral location of the ESA likely is a consequence of the differences in hydrogen bonding to ring D, with two additional hydrogen bonds from Lys and Ser to ring D in P3 and the P2KS mutant.

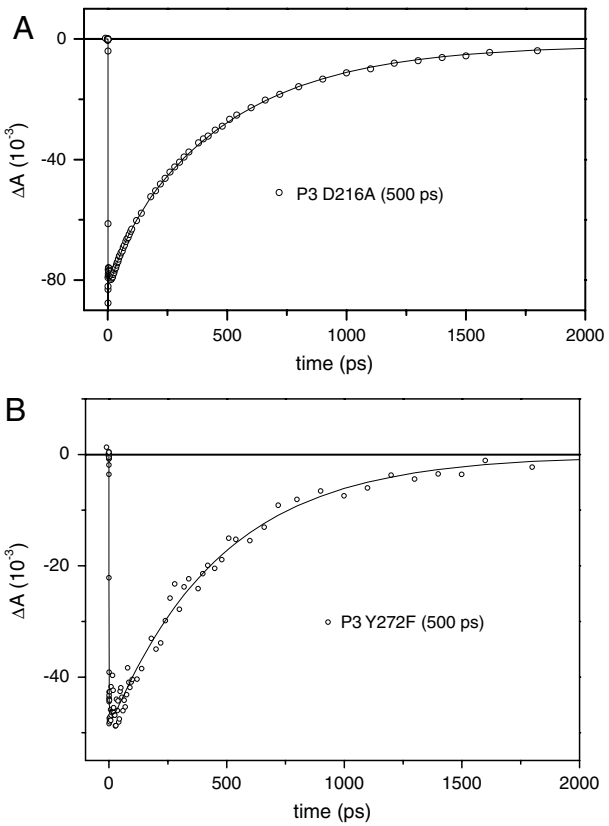

Fig. S8. Time-resolved experiment on the P3 D216A mutant (*A*) and the P3 Y272F mutant (*B*) with excitation at 680 nm and probe at 709 nm. The fits indicate an excited-state lifetime of 500 ps for both mutants.

Table S1. Rates estimated from a target analysis of the time-resolved data of P3 (upper) and P2 (lower) by using the kinetic schemes shown in Fig. 3 (P3) and Fig. S8*A* (P2).

P3 target analysis

	H_2O		D_2O		
	ps^{-1}	ps	ps^{-1}	ps	KIE
k_1	0.29	3.4	0.26	3.9	1.15
k_2	2.4×10^{-2}	42	1.89×10^{-2}	53	1.26
k_3	1.9×10^{-4}	5,400	1.7×10^{-4}	5,800	1.08
k_4	2.9×10^{-3}	350	1.95×10^{-3}	500	1.43
k_R	1.5×10^{-4}	6,600	1.5×10^{-4}	6,600	N/A*

P2 target analysis

	$H_2O\ \Phi_1 = 0.61$		$D_2O\ \Phi_1 = 0.61$		
	ps^{-1}	ps	ps^{-1}	ps	KIE
k_1	3.0	0.3	3.0	0.3	1
k_2	0.244	4.1	0.244	4.1	1
k_3	4.6×10^{-3}	220	3.9×10^{-3}	259	1.18
k_4	1.93×10^{-2}	52	1.63×10^{-2}	61	1.18
k_5	5.2×10^{-4}	1,900	5.2×10^{-4}	1,900	1
k_6	5.5×10^{-3}	180	3.8×10^{-2}	262	1.45
k_R	1.5×10^{-4}	6,600	1.5×10^{-4}	6,600	N/A*

*Not applicable.